Theoretical Study of a d^* resonance in the coupled $^3D_3$ - $^3G_3$ partial waves of nucleon-nucleon scattering

Hongxia Huang[a], Jialun Ping[a*], Chengrong Deng[b] and Fan Wang[c]
[a] *Department of Physics, and Jiangsu Key Laboratory for Numerical Simulation of Large Scale Complex Systems, Nanjing Normal University, Nanjing 210023, China*
[b] *School of Mathematics and Physics, Chongqing Jiaotong University, Chongqing 400074, China and*
[c] *Department of Physics, Nanjing University, Nanjing 210093, China*

We calculated the phase shifts of the coupled $^3D_3$ - $^3G_3$ partial waves of nucleon-nucleon scattering taking into account the $^7S_3$ $\Delta-\Delta$ channel coupling in the framework of two constituent quark models: the quark delocalization color screening model and the chiral quark model. Our results show that there is a resonance due to $^7S_3^{\Delta\Delta}$ coupling to the $^3D_3^{NN}$ and $^3G_3^{NN}$ partial waves in both of these two models, which is consistent with the d* resonance observed by WASA-at-COSY collaboration. The resonance structure in the $^3D_3^{NN}$ partial wave is remarkable, whereas in the $^3G_3^{NN}$ phase shifts there is only a small bump around the resonance energy. This result is in agreement with the recent experimental results of WASA-at-COSY Collaboration.

PACS numbers: 13.75.Cs, 12.39.Pn, 12.39.Jh, 14.20.Pt

arXiv:1404.0947v2 [nucl-th] 22 Dec 2014

I. INTRODUCTION

Recently, a narrow resonance-like structure has been observed in the reaction $pn \to d\pi^0\pi^0$ and $pn \to d\pi^+\pi^-$ at a mass $M = 2.37$ GeV with width $\Gamma \approx 70$ MeV [1–3], which indicates the existence of an $IJ^P = 03^+$ subthreshold $\Delta\Delta$ resonance, called d^* in the literature. Additional evidences had been found in the exclusive measurements of the quasi-free $pn \to pp\pi^0\pi^-$ reaction [4]. A. Pricking *et al*. suggested that if this observed resonance structure constitutes an $s-$channel resonance in the pn system, then it should cause distinctive consequences in pn scattering [5]. Then they added the resonance amplitude in the $^3D_3$ ($^3G_3$) partial wave analysis, estimated the resonance effect in pn scattering and found that the resonance effect improves considerably the description of total cross section of pn scattering and the vector analyzing power A_y exhibits the largest sensitivity to the resonance. High precision data are needed for the energy region $T_n = 1.0 - 1.3$ GeV to have a crucial test of the resonance hypothesis. Such measurements have actually been carried out very recently with the WASA detector at COSY, in which the pn analyzing power A_y was measured over a large angular range [6]. Incorporating the new A_y data into the SAID analysis produces a pole in the $^3D_3$ - $^3G_3$ partial waves as expected from the d^* resonance hypothesis.

The possibility of $IJ^P = 03^+$ dibaryon state was first proposed by Dyson and Xuong in 1964 [7], in which a bound $\Delta\Delta$ state was predicted to lie at 2350 MeV. Goldman *et al*. [8] showed that the d^* should be bound in any QCD based quark model that incorporates color confinement, hyperfine color-magnetic interaction and quark delocalization. They called it inevitable non-strange dibaryon d*. The recent three-body Faddeev equation calculation supports the existence of d^* [9]. M. Bashkanov *et al*. further pointed out that the observation of the d^* resonance state will rewarm the search of other novel six-quark configurations allowed by QCD [10]. Our former calculations showed that the $I = 0$, $J = 3$ d^* is a tightly bound six-quark system rather than a loosely bound nucleus-like system of two Δs [11–13]. Recently, our group calculated the resonance mass and decay width of the $IJ^P = 03^+$ and $IJ^P = 30^+$ $\Delta\Delta$ states and showed that the $IJ^P = 03^+$ $\Delta\Delta$ resonance is a promising candidate for the recent observed one in the so-called ABC-effect [14, 15]. However, where we only calculate the d^* resonance in the $^3D_3$ partial wave of nucleon-nucleon (NN) scattering [14]. Whether there is a resonance structure in the coupled $^3D_3$ - $^3G_3$ partial waves of nucleon-nucleon scattering as expected in Ref. [5] and the experimental observations of Ref. [6]? This article reports the results of a channel coupling calculation of the $I = 0$ NN scattering in the coupled $^3D_3$ - $^3G_3$ partial waves with and without the $^7S_3$ d^* structure.

The direct use of Quantum chromodynamics (QCD), the fundamental theory of the strong interaction, in nucleon-nucleon interaction is still out of reach of the present techniques, although the lattice QCD has made a considerable progress recently [16]. QCD-inspired quark models are still the main approach to study the baryon-baryon interaction. In our former study of the nucleon-nucleon scattering and the d^* resonance state, two quark models were used: one is the chiral quark model (ChQM) [17], in which the σ meson is indispensable to provide the intermediate-range attraction; The other is the quark delocalization color screening model (QDCSM) [11], which has been developed with the aim to understand the well-known similarities between nuclear and molecular forces despite the obvious energy and length scale differences. In this model, the intermediate-range attraction is achieved by the quark delocalization, which is like the electron percolation in the molecules.

*jlping@njnu.edu.cn, corresponding author

The color screening is needed to make the quark delocalization feasible and it might be an effective description of the hidden color channel coupling [18]. Both two models have been successfully applied to hadron spectroscopy and NN interaction. In this work, we use these two quark models to study the resonance structure in the $^3D_3$, $^3G_3$ and the coupled $^3D_3$ - $^3G_3$ partial waves of NN scattering.

The structure of this paper is as follows. A brief introduction of two quark models is given in section II. Section III devotes to the numerical results and discussions. The last section is a summary.

II. TWO QUARK MODELS

The two quark models: chiral quark model and quark delocalization color screening model, have been used in our previous work to study the NN N-hyperon interaction and dibaryon [14]. The details of two models can be found in Refs. [11, 12, 14, 17]. In the following, only the Hamiltonians and parameters are given.

A. Chiral quark model

The ChQM Hamiltonian in NN sector is

$$\begin{aligned}
H &= \sum_{i=1}^{6}\left(m_i+\frac{p_i^2}{2m_i}\right)-T_c \\
&+ \sum_{i<j}\left[V^G(r_{ij})+V^\pi(r_{ij})+V^\sigma(r_{ij})+V^C(r_{ij})\right], \\
V^G(r_{ij}) &= \frac{1}{4}\alpha_s\lambda_i\cdot\lambda_j\left[\frac{1}{r_{ij}}-\frac{\pi}{m_q^2}\left(1+\frac{2}{3}\sigma_i\cdot\sigma_j\right)\delta(r_{ij})\right. \\
&\left.-\frac{3}{4m_q^2r_{ij}^3}S_{ij}\right]+V_{ij}^{G,LS}, \\
V_{ij}^{G,LS} &= -\frac{\alpha_s}{4}\lambda_i\cdot\lambda_j\frac{1}{8m_q^2}\frac{3}{r_{ij}^3}[\mathbf{r}_{ij}\times(\mathbf{p}_i-\mathbf{p}_j)]\cdot(\sigma_i+\sigma_j), \\
V^\pi(r_{ij}) &= \frac{1}{3}\alpha_{ch}\frac{\Lambda^2}{\Lambda^2-m_\pi^2}m_\pi\left\{\left[Y(m_\pi r_{ij})-\frac{\Lambda^3}{m_\pi^3}Y(\Lambda r_{ij})\right]\right. \\
&\left.\sigma_i\cdot\sigma_j+\left[H(m_\pi r_{ij})-\frac{\Lambda^3}{m_\pi^3}H(\Lambda r_{ij})\right]S_{ij}\right\}\tau_i\cdot\tau_j, \\
V^\sigma(r_{ij}) &= -\alpha_{ch}\frac{4m_u^2}{m_\pi^2}\frac{\Lambda^2 m_\sigma}{\Lambda^2-m_\sigma^2}\left[Y(m_\sigma r_{ij})-\frac{\Lambda}{m_\sigma}Y(\Lambda r_{ij})\right] \\
&+ V_{ij}^{\sigma,LS}, \qquad (1) \\
V_{ij}^{\sigma,LS} &= -\frac{\alpha_{ch}}{2m_\pi^2}\frac{\Lambda^2}{\Lambda^2-m_\sigma^2}m_\sigma^3\left[G(m_\sigma r_{ij})-\frac{\Lambda^3}{m_\sigma^3}G(\Lambda r_{ij})\right] \\
&[\mathbf{r}_{ij}\times(\mathbf{p}_i-\mathbf{p}_j)]\cdot(\sigma_i+\sigma_j),
\end{aligned}$$

$$\begin{aligned}
V^C(r_{ij}) &= -a_c\lambda_i\cdot\lambda_j(r_{ij}^2+V_0)+V_{ij}^{C,LS}, \\
V_{ij}^{C,LS} &= -a_c\lambda_i\cdot\lambda_j\frac{1}{8m_q^2}\frac{1}{r_{ij}}\frac{df(r_{ij})}{dr_{ij}}[\mathbf{r}_{ij}\times(\mathbf{p}_i-\mathbf{p}_j)] \\
&\cdot(\sigma_i+\sigma_j), \qquad f(r_{ij})=r_{ij}^2, \\
S_{ij} &= \frac{(\sigma_i\cdot\mathbf{r}_{ij})(\sigma_j\cdot\mathbf{r}_{ij})}{r_{ij}^2}-\frac{1}{3}\,\sigma_i\cdot\sigma_j.
\end{aligned}$$

Where S_{ij} is quark tensor operator, $Y(x)$, $H(x)$ and $G(x)$ are standard Yukawa functions, T_c is the kinetic energy of the center of mass. All other symbols have their usual meanings.

B. Quark delocalization color screening model

The Hamiltonian of QDCSM has the same form as Eq.(1), but without σ meson exchange and a phenomenological color screening confinement potential is used,

$$\begin{aligned}
V^C(r_{ij}) &= -a_c\lambda_i\cdot\lambda_j[f(r_{ij})+V_0]+V_{ij}^{C,LS}, \\
f(r_{ij}) &= \begin{cases} r_{ij}^2 & \text{if } i,j \text{ occur in the same baryon orbit,} \\ \frac{1-e^{-\mu r_{ij}^2}}{\mu} & \text{if } i,j \text{ occur in different baryon orbits.} \end{cases} \qquad (2)
\end{aligned}$$

Here, μ is the color screening constant to be determined by fitting the deuteron mass. The quark delocalization in QDCSM is realized by replacing the left- and right-centered Gaussian functions, the single-particle orbital wave functions in the usual quark cluster model,

$$\phi_\alpha(\vec{S}_i) = \left(\frac{1}{\pi b^2}\right)^{3/4} e^{-\frac{1}{2b^2}(\vec{r}_\alpha-\vec{S}_i/2)^2} \qquad (3)$$

$$\phi_\beta(-\vec{S}_i) = \left(\frac{1}{\pi b^2}\right)^{3/4} e^{-\frac{1}{2b^2}(\vec{r}_\beta+\vec{S}_i/2)^2}. \qquad (4)$$

with delocalized ones,

$$\begin{aligned}
\psi_\alpha(\vec{S}_i,\epsilon) &= \left(\phi_\alpha(\vec{S}_i)+\epsilon\phi_\alpha(-\vec{S}_i)\right)/N(\epsilon), \\
\psi_\beta(-\vec{S}_i,\epsilon) &= \left(\phi_\beta(-\vec{S}_i)+\epsilon\phi_\beta(\vec{S}_i)\right)/N(\epsilon), \qquad (5) \\
N(\epsilon) &= \sqrt{1+\epsilon^2+2\epsilon e^{-S_i^2/4b^2}}.
\end{aligned}$$

The parameters of two models are fixed by baryon and deuteron properties and/or nucleon-nucleon scattering phase shifts, they are listed in Table I.

C. The calculation method

To calculate the NN scattering phase shifts and resonance states, the well developed resonating group method (RGM) is used. The details of RGM can be found in Ref.[20]. Here only the necessary equations are given. In

TABLE I: Parameters of quark models

	ChQM	QDCSM
$m_{u,d}$(MeV)	313	313
b(fm)	0.518	0.518
a_c(MeV fm^{-2})	46.938	56.755
V_0(fm^2)	-1.297	-0.5279
μ(fm^{-2})	–	0.45
α_s	0.485	0.485
m_π(MeV)	138	138
α_{ch}	0.027	0.027
m_σ(MeV)	675	–
Λ(fm^{-1})	4.2	4.2

RGM, the multiquark wave functions are approximated by the cluster wave functions, the internal motions of clusters are frozen and the relative motion wave-function $\chi(\boldsymbol{R})$ satisfies the following RGM equation

$$\int H(\boldsymbol{R''},\boldsymbol{R'})\chi(\boldsymbol{R'})d\boldsymbol{R'} = E\int N(\boldsymbol{R''},\boldsymbol{R'})\chi(\boldsymbol{R'})d\boldsymbol{R'}, \tag{6}$$

where

$$\left\{\begin{array}{c} H(\boldsymbol{R''},\boldsymbol{R'}) \\ N(\boldsymbol{R''},\boldsymbol{R'}) \end{array}\right\} = \langle\mathcal{A}[\phi_1\phi_2\delta(\boldsymbol{R}-\boldsymbol{R''})]|\left\{\begin{array}{c} H \\ 1 \end{array}\right\} |\mathcal{A}[\phi_1\phi_2\delta(\boldsymbol{R}-\boldsymbol{R'})]\rangle\,. \tag{7}$$

where ϕ_1,ϕ_2 are the internal wavefunctions of two clusters. $\mathcal{A}=1+\mathcal{A}'$ is the anti-symmetrization operator and has the properties, $\mathcal{A}H=H\mathcal{A}$, $\mathcal{A}^2=\mathcal{A}$. With this properties, the RGM equation can be written as an integro-differential equation

$$\left[\frac{\nabla^2_{\boldsymbol{R''}}}{2\mu}-V^D(\boldsymbol{R''})+E_{CM}\right]\chi(\boldsymbol{R''}) = \int W_L(\boldsymbol{R''},\boldsymbol{R'})\chi(\boldsymbol{R'})d\boldsymbol{R'}, \tag{8}$$

where $E_{CM}=E-E_{int}$ is the kinetic energy of the relative motion, and W_L is the whole exchange kernel

$$W_L(\boldsymbol{R''},\boldsymbol{R'}) = H^E(\boldsymbol{R''},\boldsymbol{R'}) - EN^E(\boldsymbol{R''},\boldsymbol{R'}), \tag{9}$$

where the exchange kernels of the hamiltonian and overlap are defined as

$$\begin{aligned} H^E(\boldsymbol{R''},\boldsymbol{R'}) &= \langle\phi_1\phi_2\delta(\boldsymbol{R}-\boldsymbol{R''})|H|\mathcal{A}'[\phi_1\phi_2\delta(\boldsymbol{R}-\boldsymbol{R'})]\rangle, \\ N^E(\boldsymbol{R''},\boldsymbol{R'}) &= \langle\phi_1\phi_2\delta(\boldsymbol{R}-\boldsymbol{R''})|\mathcal{A}'|\phi_1\phi_2\delta(\boldsymbol{R}-\boldsymbol{R'})\rangle. \end{aligned} \tag{10}$$

III. THE RESULTS AND DISCUSSIONS

In order to study the resonance effects in the NN scattering observables, we calculate the NN scattering phase shifts with and without the $\Delta\Delta$ state, respectively. All the coupled channels are listed in Table II.

TABLE II: The channels involved in the calculations.

sc.	2cc.	3cc.
$^3D_3^{NN}$	$^3D_3^{NN}+^7S_3^{\Delta\Delta}$	$^3D_3^{NN}+^3G_3^{NN}+^7S_3^{\Delta\Delta}$
$^3G_3^{NN}$	$^3G_3^{NN}+^7S_3^{\Delta\Delta}$	
	$^3D_3^{NN}+^3G_3^{NN}$	

We first discuss the results from QDCSM. The results are shown in Fig. 1. The experimental information used for the comparison is the partial waves solution SP07 [21].

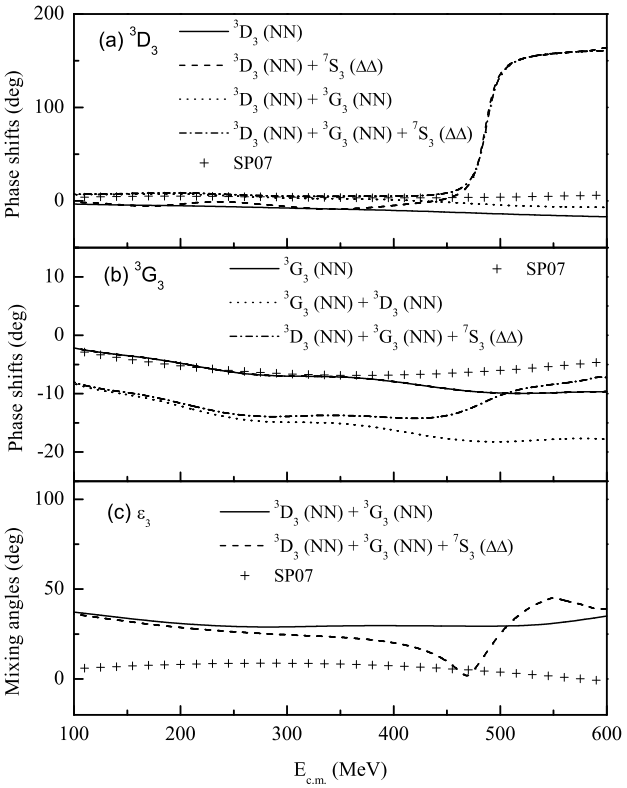

FIG. 1: $^3D_3^{NN}$ and $^3G_3^{NN}$ phase shifts including their mixing angles ε_3 in QDCSM.

Firstly, we do a single channel calculation for the phase shifts of $^3D_3$ and $^3G_3$ partial waves of NN scattering, which are denoted by the solid lines in Figs. 1(a) and 1(b), respectively. No resonance structure can be found in both two channels as expected. Both the $^3D_3^{NN}$ and $^3G_3^{NN}$ scattering phase shifts fit the SP07 data well, especially for the low energy scattering, $E_{CM}<400$ MeV. For $^3G_3^{NN}$ partial wave, the phase shifts at high energy, $E_{CM}>400$, deviate from the SP07 data, which rise up slowly.

Secondly, two-channel coupling calculations are per-

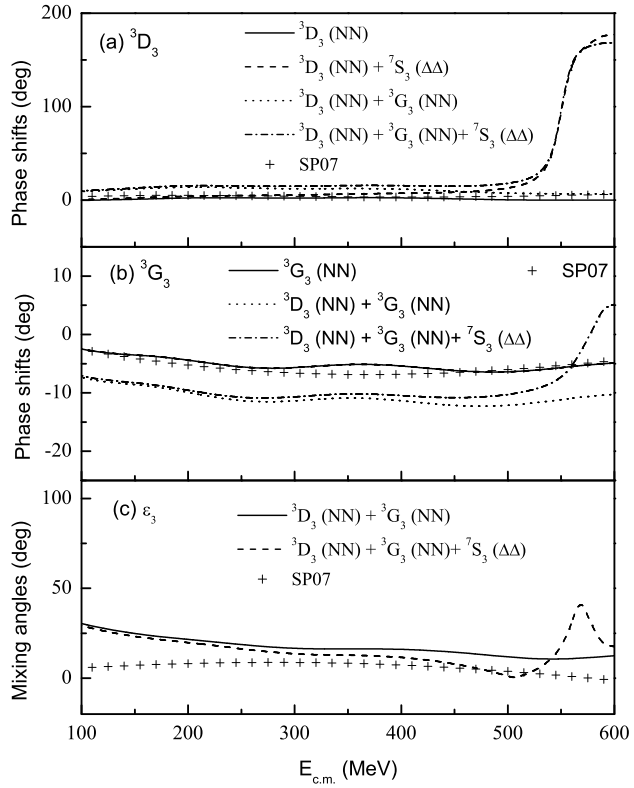

FIG. 2: $^3D_3^{NN}$ and $^3G_3^{NN}$ phase shifts including their mixing angles ε_3 in ChQM.

formed. The state $^7S_3^{\Delta\Delta}$ is added in the phase shift calculations of the $^3D_3^{NN}$ and $^3G_3^{NN}$ partial waves of NN scattering. The results are shown in Fig. (1a) by the dashed line. From Fig. 1(a) we can see that the channel coupling of $^7S_3^{\Delta\Delta}$ has minor effects on phase shifts of $^3D_3^{NN}$ for $E_{CM} < 400$ MeV, but it causes that the phase shifts rise through $\pi/2$ at a resonance mass ~ 2360 MeV. For $^3G_3^{NN}$ phase shifts, there is no coupling between $^3G_3^{NN}$ and $^7S_3^{\Delta\Delta}$, so the channel coupling phase shifts is exactly the same as the single channel ones. The reason for this is that, if only the two-body interactions are used, as our two quark models assumed, the two-body tensor interaction can only induce a $\Delta L = 2$ change at a time. Therefore, the $^7S_3^{\Delta\Delta}$ cannot couple to $^3G_3^{NN}$ directly, and the $^7S_3^{\Delta\Delta}$ state must go through the intermediate $^3D_3^{NN}$ channel to affect the $^3G_3^{NN}$ channel. To verify this point, we do the following calculations.

Thirdly, we calculate the phase shifts of the coupled $^3D_3^{NN}$ and $^3G_3^{NN}$ partial waves. The phase shifts of $^3D_3^{NN}$ and $^3G_3^{NN}$ scattering are denoted by the dotted lines in Fig. 1(a) and Fig.1(b), respectively. Obviously, there is no resonance structure in any channel as expected. By coupling to $^3G_3^{NN}$, the phase shifts of $^3D_3^{NN}$ fit the SP07 data better than the pure $^3D_3^{NN}$ does. However, the coupling to $^3D_3^{NN}$ push down the phase shifts of $^3G_3^{NN}$ from the SP07 data a little.

Fourthly, we include the $^7S_3^{\Delta\Delta}$ state in the phase shift calculation of coupled $^3D_3^{NN}$ and $^3G_3^{NN}$ partial waves. The phase shifts of $^3D_3^{NN}$ and $^3G_3^{NN}$ are denoted by the dash-dotted lines in Figs. 1(a) and 1(b), respectively. We find that there is a remarkable resonance structure in the $^3D_3^{NN}$ partial wave, whereas in the $^3G_3^{NN}$ phase shifts, there is only a small bump around the resonance energy. This result is consistent with the recent observations of the WASA-at-COSY Collaboration, in which $^3D_3^{NN}$ wave obtained a typical resonance shape, whereas the $^3G_3^{NN}$ wave changed less dramatically [6]. In addition, we can see the effect of $^7S_3^{\Delta\Delta}$ on the phase shifts of $^3G_3^{NN}$ clearly. It proceeds through the intermediate channel $^3D_3^{NN}$.

Finally, we give the mixing angles of the coupled $^3D_3^{NN}$ and $^3G_3^{NN}$ partial waves in Fig. 1(c). The solid (dashed) curves denote the result without (with) the resonance state $^7S_3^{\Delta\Delta}$ in the coupled $^3D_3^{NN}$ and $^3G_3^{NN}$ partial waves. A valley and a peak around the resonance energy appear by including the resonance state $^7S_3^{\Delta\Delta}$.

Then we do the same calculations by using another quark model ChQM. The results are shown in Fig. 2. The meaning of the curves are the same as those in Fig. 1. From Fig. 2, we find that all the results are consistent with the ones from QDCSM. Only the resonance mass moves to ~ 2410 MeV, which is higher than the observed one and that in QDCSM by $\sim 30(50)$ MeV.

In order to compare our results with the recent observations of the WASA-at-COSY Collaboration [6], we show the $^3D_3^{NN}$ and $^3G_3^{NN}$ amplitudes including their mixing amplitude ε_3 for the two quark models in Fig. 3. From Fig. 3(a), we can see that the $^3D_3^{NN}$ partial wave obtains a typical resonance structure in both models, which is consistent with Ref. [6]. But the resonance mass is ~ 2360 MeV in QDCSM, ~ 2410 MeV in ChQM, a little lower and higher than ~ 2380 MeV in Ref. [6]. From Fig. 3(b), we can see that both quark models give similar amplitudes of the $^3G_3^{NN}$ partial wave. Although there are small structures around the resonance energy, the theoretical results are different from the experimental ones. The real part of amplitude in model calculation rises a little after the resonance energy, whereas the experimental ones fall down. For imaginary part, we have a total inversed results. The amplitude falls down a little in theoretical calculation and rises in experimental measurement [6]. For the mixing amplitude ε_3 as shown in Fig. 3(c), the real parts of the partial wave in two quark models are consistent with that of Ref. [6], there is a valley around the resonance energy, whereas the imaginary parts in both models are different from that of Ref. [6].

IV. SUMMARY

In conclusion, inspired by the recent results of the WASA-at-COSY Collaboration, where they did a partial wave analysis including the new np scattering data and

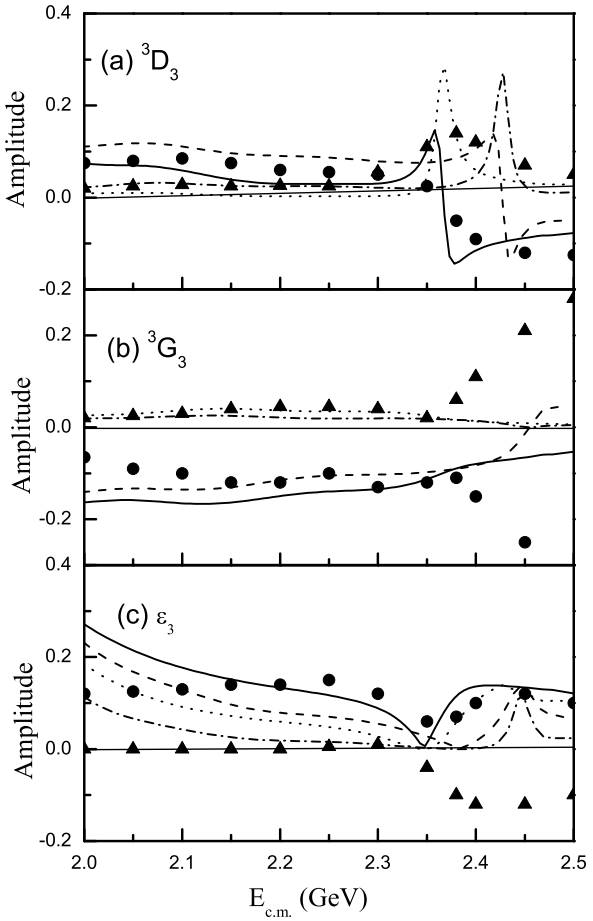

FIG. 3: ${}^3D_3^{NN}$ and ${}^3G_3^{NN}$ amplitudes including their mixing amplitude ε_3 in two quark models. Solid (dotted) curves give the real (imaginary) part of partial-wave amplitudes in QDCSM, whereas the dashed (dash-dotted) curves represent the real (imaginary) part of partial wave amplitudes in ChQM. Results from Ref. [6] are shown as solid circles (real part) and solid triangles (imaginary part).

found a resonance pole in the coupled ${}^3D_3$ and ${}^3G_3$ partial waves as expected from the d^* resonance hypothesis, we study the d^* resonance structure in the coupled ${}^3D_3$ - ${}^3G_3$ partial waves of NN scattering in the framework of QDCSM and ChQM. Our results show that there is indeed a resonance in the coupled ${}^3D_3^{NN}$ - ${}^3G_3^{NN}$ partial waves due to the coupling of the ${}^7S_3^{\Delta\Delta}$ state, which is consistent with the existence of the d^* resonance. The resonance structure in the ${}^3D_3^{NN}$ partial wave is remarkable, whereas in the ${}^3G_3^{NN}$ phase shifts there is only a small bump around the resonance energy. This result is also consistent with the recent observations of the WASA-at-COSY Collaboration [6]. From our calculation, one can see that the small bump in the phase shifts of ${}^3G_3$ partial wave of NN scattering is an indication of the existence of a resonance, ${}^7S_3^{\Delta\Delta}$.

Moreover, QDCSM and ChQM obtained similar results. Only the mass and decay width of the d^* resonance in QDCSM are smaller than that in ChQM. It shows once again the consistency of these two quark models even though they have different intermediate-range attraction mechanisms. Our former study has shown that by including the hidden-color channels in ChQM, the resonance masses are lowered by 10-20 MeV [14, 15]. This fact inferred that the quark delocalization and color screening used in QDCSM might be an effective description of the hidden color channel coupling.

For the partial wave amplitudes, the behavior of the theoretical calculated ones are different from the measured ones. The further study is needed.

Acknowledgment

This work is supported partly by the National Science Foundation of China under Contract Nos. 11205091, 11035006 and 11175088.

[1] M. Bashkanov *et al* (CELSIUS-WASA Collaboration), Phys. Rev. Lett. **102**, 052301 (2009).
[2] P. Adlarson *et al* (WASA-at-COSY Collaboration), Phys. Rev. Lett. **106**, 242302 (2011).
[3] P. Adlarson *et al* (WASA-at-COSY Collaboration), Phys. Lett. **B721**, 229 (2013).
[4] P. Adlarson *et al* (WASA-at-COSY Collaboration), Phys. Rev. **C88**, 055208 (2013).
[5] A. Pricking, M. Bashkanov, H. Clement, arXiv:1310.5532v1 [nucl-ex].
[6] P. Adlarson *et al* (WASA-at-COSY Collaboration), Phys. Rev. Lett. **112**, 202301 (2014).
[7] F. J. Dyson and N. H. Xuong, Phys. Rev. Lett. **13**, 815 (1964).
[8] T. Goldman, K. Maltman, G. J. Stephenson, K. E. Schmidt and F. Wang, Phys. Rev. **C39**, 1889 (1989).
[9] A. Gal and H Garcilazo, Phys. Rev. Lett. **111**, 172301 (2013).
[10] M. Bashkanov, S. J. Brodsky and H. Clement, Phys. Lett. B **727**, 438 (2013).
[11] F. Wang, G. H. Wu, L. J. Teng and T. Goldman, Phys. Rev. Lett. **69**, 2901 (1992).

[12] F. Wang, J. L. Ping, G. H. Wu, L. J. Teng and T. Goldman, Phys. Rev. **C51**, 3411 (1995); J. L. Ping, H. R. Pang, F. Wang and T. Goldman, Phys. Rev. **C65**, 044003 (2002); J. L. Ping, F. Wang and T. Goldman, Nucl. Phys. **A657**, 95 (1999); J. L. Ping, F. Wang and T. Goldman, Nucl. Phys. A **688**, 871 (2001).

[13] H. R. Pang, J. L. Ping, F. Wang and T. Goldman, Phys. Rev. **C65**, 014003 (2001).

[14] J. L. Ping, H. X. Huang, H. R. Pang, F. Wang and C. W. Wong, Phys. Rev. **C 79**, 024001 (2009).

[15] H. X. Huang, J. L. Ping and F. Wang, Phys. Rev. **C 89**, 034001 (2014).

[16] S. Aoki, Eur. J. Phys. A **49**, 81 (2013) and refernces therein.

[17] A. Valcarce, H. Garcilazo, F. Fernandez and P. Gonzalez, Rep. Prog. Phys. **68**, 965 (2005) and references therein.

[18] H. X. Huang, P. Xu, J. L. Ping and F. Wang, Phys. Rev. **C 84**, 064001 (2011).

[19] M. M. Xu, M. Yu and L. S. Liu, Phys. Rev. Lett. **100**, 092301 (2008).

[20] M. Kamimura, Supp. Prog. Theo. Phys. **62**, 236 (1977).

[21] R. A. Arndt, W. J. Briscoe, I. I. Strakovsky and R. L. Workman, *Phys. Rev. C* **76**, 025209 (2007).